

Supplementary information

Fang et al.

Polyvalent mRNA vaccination elicited potent immune response to monkeypox virus surface antigens

Inventory of supporting information

Supplementary discussion

Methods and Materials

References

Reporting summary

Supplementary figures and legends

Supplemental source data and statistics

Supplementary table 1. Sequence and Genbank ID of MVA and MPXV antigens

Supplementary table 2. Structure and biophysical property of MPXV antigens

Both supplementary tables are included in file “20220827_supplementary_tables.xlsx”.

Source Data and Statistics

Provided in an excel file, “20230215_MPXVac_data_summary.xlsx”.

Supplementary discussion

Introduction

To date (December 28, 2022), the ongoing monkeypox outbreak has led to more than 83,000 confirmed cases and ~240 deaths in over 110 countries. Because of its fast spread, world health organization declared the monkeypox (Mpox) outbreak a global public-health emergency on July 23rd. Vaccination is the ultimate approach to prevent infectious disease outbreak from developing into a global pandemic. Replication-deficient modified vaccinia Ankara (MVA) vaccine, JYNNEOS is the approved and preferred vaccine for monkeypox due to less side effects and contraindications compared to ACAM2000. A retrospective study recently reported evidence of asymptomatic or undiagnosed monkeypox cases during early stage of monkeypox outbreak suggesting that asymptomatic cases fueled this epidemic, and symptom-based testing and quarantining may not suffice to contain monkeypox outbreak¹. In addition to testing and quarantining, an efficient measure to contain monkeypox virus (MPXV) transmission is the use of monkeypox vaccines for high-risk groups and close contacts of patients². As the monkeypox outbreak grows rapidly, the demand for monkeypox vaccines surges drastically and many countries are facing the vaccine supply shortage.

Replication-deficient modified vaccinia Ankara (MVA) vaccine, JYNNEOS (commercial name in U.S., IMVANEX in Europe and IMVAMUNE in Canada) is the approved and preferred vaccine for monkeypox due to less side effects and contraindications compared to ACAM2000, which is a replication-competent vaccinia vaccine also available for use against monkeypox²⁻⁴. The authorization of JYNNEOS and ACAM2000 is based on 1) a phase 3 trial assessing neutralizing antibody response to vaccinia virus in vaccinees of MVA and ACAM2000⁵; and 2) a MPXV challenge experiment in macaques showing 100% protection after two doses of MVA or one dose of ACAM2000 injection⁶. A series of clinical trials and cohort studies are underway to evaluate MVA vaccine's efficacy, safety and protection durability⁷.

The mRNA vaccine technology has catalyzed the tremendous success of COVID mRNA vaccine, which has proven to be safe and effective across the globe. It is a versatile platform that can be adopted to develop mRNA vaccines against SARS-CoV-2 evolving variants^{8, 9} and other infectious diseases, including monkeypox. Although MVA-based vaccine has less side effect than ACAM2000, its ≥ 3 grade adverse event rate is 7.7% in recipients⁵. In contrast, the ≥ 3 grade adverse event rate of COVID mRNA vaccine is similar to placebo group (1.5% in vaccine group vs. 1.3% in placebo group)¹⁰. The MVA vaccine contains around 200 proteins, many of which are not immunogenic¹¹ and infection of MVA live virus likely triggers

inflammation and related side effects. Removal of undesired components in MPXV vaccines would improve its safety profile, which is the case for MVA that lost large fragments of genome and replication capability in human during attenuation¹². In addition, the manufacturing of mRNA vaccine is easily scalable by biochemical reactions. These features together make mRNA vaccine promising to quickly fill the gap between vaccine supply and demand during a disease outbreak.

Proteomic analysis of antibody response to MPXV infection and vaccinia vaccination revealed a number of immunodominant envelope proteins¹¹. Among them, vaccinia A27L¹³, D8L^{13,14}, H3L¹⁵, L1R¹⁶, A33R¹⁷ and B5R¹⁸ have been identified as targets of neutralizing antibodies. Polyvalent DNA vaccines combining vaccinia antigens A27L, D8L, L1R, A33R and B5R protected macaques and mice from lethal MPXV challenge¹⁹. The MPXV equivalent antigens of vaccinia A27L, D8L, L1R, A33R and B5R are A29L, E8L, M1R, A35R and B6R respectively¹³. Among them, A35R and B6R are surface proteins of enveloped virion (EV) and the remaining three proteins are surface antigens of mature virion (MV).

Results

The 2022 MPXV variants causing the outbreak form the lineage B.1 branch that belongs to MPXV clade 3²⁰. Because of high sequence identity, immunity elicited by attenuated vaccinia vaccine can provide protection from monkeypox and smallpox. Both MPXV and vaccinia virus belong to Orthopoxvirus genus, which also includes variola virus, the pathogen of smallpox. Sequence alignment of MPXV 2022 and MVA revealed that M1R antigen is largely conserved between MPXV and MVA, while the other four antigens contain 4-6% substitutions. Among these substitutions, K149E in A35R and T144A, S65T, L66I, R67H in E8L are located on reported neutralizing antibody interface^{14, 17} and are speculated to lower affinity of neutralizing antibodies (Supplementary information, Fig. 2). Interestingly, to prevent host cell interaction, the neutralizing antibody of E8L recognizes and blocks the ligand binding site which contains a large positive-charge patch to accommodate the negative charged chondroitin sulfate ligand of host cells (Supplementary information, Fig. 2).

Among the five MPXV antigens, A35R showed a cellular distribution most similar to spike, while the A29L, that lacks transmembrane domain, was mainly diffused in cytosol. Interestingly, the expression of A29L translocated the membrane dye, CellBrite-Green from membrane to cytosols. B6R displayed an enrichment in perinuclear structures which include a perinuclear ring and a network-like structure expanding from the ring. The network-like structure was further confirmed by utilizing computational

deconvolution to enhance the contrast and resolution of confocal microscopy (Fig. 1b). E8L had a high enrichment in plasma membrane, but a significant cytosol fraction could still be observed. M1R associated with plasma membrane, was prone to aggregate and led to a more rounded morphology in comparison to the elongated morphology in other samples (Supplementary information, Fig. 4).

Discussion

The immense success of COVID mRNA vaccine and global outbreak of Mpox have facilitated the development of Mpox mRNA vaccine. MPXV is a DNA virus of the genus Orthopoxvirus (poxvirus). Research of poxvirus vaccine dates back to late 18th century when the vaccination against smallpox was discovered by Dr. Edward Jenner²¹. It marks a millstone of vaccine research and lays the groundwork for global eradication of smallpox in 1970s. Development of newer poxvirus vaccines primarily focuses on higher safety, which is crucial for immunocompromised patients as live poxvirus inoculation would cause more severe side effects in these patients. To prevent future poxvirus outbreak, U.S. government strategically stockpiled 200 million doses of ACAM2000²², which replaced the first-generation smallpox vaccine Dryvax that has a questionable safety profile. However, ACAM2000 vaccination was later found associated with high rate of myopericarditis, foreshadowing the need to update this strategic stockpile once again. A pan-poxvirus mRNA vaccine with excellent safety profile and broad targeting spectrum could be a key to prevent Mpox and/or other poxvirus outbreaks. This need opens up opportunities for the development of pan-poxvirus mRNA vaccine that target multiple poxvirus species with high potency.

What's more, the immunocompromised patients are high-risk groups of Mpox infection who are more likely to need vaccination. The COVID mRNA vaccine has been administered in millions of people with minimal adverse events, establishing a reliable safety profile of mRNA delivery platform. However, it remains an unanswered question that whether immunization with key MPXV mRNA antigens is safe in vivo. Our preclinical study here aims to design a multivalent Mpox mRNA vaccine and evaluate its immunogenicity as well as safety in vivo.

Here we report a multivalent Mpox mRNA vaccine candidate, MPXVac-097 which encodes five key MPXV antigens in tandem and compare its immunogenicity with single antigen LNP mRNA as well as Mix-5, equal mass mixture of single antigen LNP mRNAs. Our proof-of-principle study demonstrates that mRNA vaccine against MPXV can elicit potent antibody and T cell responses against viral antigens, and it is well-tolerated in mice. MPXVac-097 vaccination elicited T cell clonal expansion and broadly neutralizing antibodies that

cross neutralized cowpox, vaccinia virus and MPXV. The MPXV antigens stimulated MPXV-specific T cell responses in animals vaccinated with MPXVac-097. Compared to single antigen LNP mRNA, antigen co-expression in MPXVac-097 and Mix-5 led to higher antibody titers against E8L and A35R respectively, while single antigen LNP mRNAs induced higher antibody titers against A29L and B6R, implying an interplay between MPXV antigens that regulates their immunogenicity in vivo. MPXVac-097 immunization elicited a binding and neutralizing antibody response comparable to Mix-5 LNP mRNA. Given its simpler production procedure and comparable immunogenicity, the tandem co-expression of Mpox antigens by MPXVac-097 remains an attractive direction for Mpox mRNA vaccine development.

Characterization of antigen expression and surface display reveals distinct cellular localization of five key MPXV antigens. BA.5 spike as a control was predominantly localized on plasma membrane, which was visualized by tagging its C terminus with mScarlet and quantified by tagging its extracellular end with flag. The flag tag enables quantification of different antigens using the same anti-flag antibody with high specificity and low background. The whole-cell or total anti-flag staining confirms stable expression of all five MPXV antigens in cells. The dual staining represents cells expressing surface flag (PE positive, fixed) and total flag (Alexa-488 positive in permeabilizing conditions, supplementary information, Fig. S8). Since the surface flag is bound to PE anti-flag antibody and fixed or cross-linked by paraformaldehyde after surface staining, the majority of alexa-488 anti-flag antibody would label the intracellular flag in this dual staining experiment. However, it is possible that a small portion of alexa-488 would still bind to remaining unbound flag on surface. For this reason, we still use the term “total or whole-cell flag” for alexa 488 signal. In contrast to dual staining, the single-step staining after fixation and permeabilization would label total flag including surface flag and intracellular flag.

The positive results of surface staining confirm the ectodomain side of each antigen and show a higher surface display of A35R and E8L, which is associated with their plasma membrane localization in cells and higher immunogenicity in vivo. However, the surface fraction of all five MPXV antigens was lower than that of spike antigen, which points out a future direction of antigen optimization to enhance their surface localization. The M1R antigen was found prone to aggregate under confocal microscope and it is difficult to induce anti-M1R antibody using M1R mRNA LNP. Because the M1R antigen was sandwiched between A35R and E8L on the same mRNA transcript, its expression level would be comparable to A35R and E8L. The delayed increase of M1R antibody titer may stem from the difference of antigen immunogenicity, stability or surface display. Gilchuk and colleagues showed that 100% of monoclonal M1R antibodies

sampled from patients were neutralizing and could broadly cross react with Mpox, cowpox and vaccinia virus²³, suggesting that M1R is a primary target of neutralizing antibodies. Sequence optimization of M1R to improve its stability and surface display may also increase its immunogenicity in vivo.

Methods and Materials

Methods

Institutional approval

All animal work was performed under the guidelines of Yale University Institutional Animal Care and Use Committee (IACUC) with approved protocols (Chen 2020-20358; Chen 2021-20068; Lucas 2021-10365). All recombinant DNA (rDNA) and biosafety work were performed under the guidelines of Yale Environment, Health and Safety (EHS) Committee with approved protocols (Chen 18–45, 20–18, and 20–26; IA\10047\10). This study does not directly involve human materials. The three poxvirus species including cowpox, mpox and vaccinia virus were purchased from BEI and delivered as cell lysates without involving identifiable human materials. The Yale Human Research Protection Program Institutional Review Board (IRB) determined that using virus isolates from de-identified human samples were not considered research involving human participants.

Plasmid cloning

The MPXV antigen amino acid sequences used in the mRNA vaccine design were based on the genome of confirmed monkeypox case identified in Massachusetts in May, 2022 (Genbank ON563414.3)^{20, 24}. The five antigen cDNAs were codon optimized, synthesized and inserted to mRNA vector with 5', 3' UTRs and poly A tail as flanking sequences. The MPXVac-097 mRNA vaccine vector was cloned through connecting five antigen cDNAs with 2A linkers as shown in Fig. 1a. A reporter vector with GFP appended to the 3' end of the mRNA vaccine vector, MPXV-GFP, was designed to validate the successful translation of mRNA in mammalian cells (Supplementary information, Fig. S3). The mScarlet tag was added to the C-term of each Mpox antigen and flag tag was added to the ectodomain end of each antigen after the signal peptide if any.

SWISS homology modeling

Homologs of four out of five MPXV antigens were found in PDB database and were used to build the homology structures on SWISS homology-modeling server ([SWISS-MODEL \(expasy.org\)](https://swiss-model.expasy.org/)). The homology model was visualized in Pymol and was used to display neutralizing antibody epitopes and sites that are different between monkeypox and MVA.

Cell Culture

HEK293T cells (ATCC, CRL-3216) were cultured in Dulbecco's modified Eagle's medium (DMEM, Thermo fisher) with 10% heat-inactivated fetal bovine serum (FBS, Hyclone). Cells were split every other day at a split ratio of 1:3 or when confluency reaches over 95%.

MPXV antigen expression in 293T cells

The Lipo3000 transfection system (Thermo Fisher, Cat. No. L3000015) was applied to transfect 293T cells with various reporter vectors that contain single or five MPXV antigens in tandem and a N-term or C-term GFP, flag or mScarlet tags. The 293T cells were seeded on the 6-well or 12-well plates one day before transfection and transfection was performed according to manufacture's protocol. After overnight incubation with transfecting reagents, media was removed and replaced with fresh media. Two days after transfection, cells were imaged under fluorescence microscope and were subsequently subject to flow cytometry for quantification of cells co-expressing five monkeypox antigens and GFP.

Confocal microscopy

One day before imaging, the 293T cells expressing mScarlet tagged antigens were transferred to 35 mm Dish with No. 1.5 Coverslip (VWR, 10810-054). Live cells were directly imaged on SP8 or Stellaris confocal microscope with a 63X/1.40NA objective (Leica Microsystems) at room temperature. CellBrite-Green (Thomas, #30021) and Hoechst 33342 (BD, 561908, 5 µg/ml final concentration) were incubated with live cells at 37 degree for 20-30min to stain cell membrane and nucleus respectively. After staining, cells were washed with DMEM with 10% FBS once and maintained in DMEM with 10% FBS. For confocal images with deconvolution, a z stack centered at the focal plane of interest was taken. The z stack was then processed by LIGHTNING (Leica Microsystems) for deconvolution.

Cell surface MPXV antigen staining using mice plasma antibody

The same lipo3000 transfection approach was also applied to express individual MPXV antigen in 293T cells. The 293T cells expressing MPXV antigen were trypsinized, washed with 2% FBS in PBS once and resuspended in flow cytometry staining buffer (Thermo Fisher, Cat. No. 00-4222-26). Resuspended cells were incubated on ice for 20 min with 1:100 diluted plasma from mice vaccinated with two doses of MPXV LNP-mRNA. After incubation, cells were washed once with flow cytometry staining buffer and incubated on ice for 20 min with 1:100 diluted anti-mouse IgG antibody conjugated to PE fluorophore (Thermo Fisher, Cat. No. P-852). After the final wash with flow staining buffer, PE-positive cells were detected by flow

cytometry using Attune focusing cytometer (Attune NxT Software v3.1). FlowJo v.10.7.1 was used for flow cytometry data analysis.

In vitro mRNA transcription and lipid nanoparticle preparation

To produce mRNA, the MPXVac-097 vaccine candidate construct, pZF97 encoding five MPXV antigens in tandem flanked by 5' and 3' hemoglobin subunit UTRs and bGH poly A was in vitro transcribed from linear DNA template using HiScribe T7 ARCA mRNA kit (NEB, Cat. No. E2060S) with 50% replacement of uridine by N1-methyl-pseudouridine (Tirlink, Cat. No. N-1081-5). The transcribed mRNA was purified using Monarch RNA Cleanup Kits (NEB, Cat. No. T2040L) and kept in -20 until further use.

The prepared mRNA was diluted in 25mM sodium acetate buffer at pH 5.2 and mixed with lipid mixture in ethanol using NanoAssemblr[®] Ignite[™] instrument (Precision Nanosystems). The lipid mixture is composed of ALC-0315, ALC-0159, DSPC and cholesterol at a mixing ratio as previously described^{8,9}. The MPXV LNP-mRNA buffer was exchanged to phosphate buffered saline (PBS) using 100kDa Amicon filter (Macrosep Centrifugal Devices 100 K, 89131-992). The mRNA encapsulation rate and mRNA concentration were determined by Quant-iT[™] RiboGreen[™] RNA Assay (Thermo Fisher). The size distribution of LNP-mRNA sample was characterized by dynamic light scattering (DynaPro NanoStar, Wyatt, WDPN-06). 8% sucrose was added to the final LNP mRNA sample before storing it in -80 freezer.

Mouse immunization

8-10 week-old female C57BL/6Ncr mice purchased from Charles River were vaccinated with three doses of 5 µg or 8 µg MPXVac-097 LNP-mRNA vaccine candidate on day 0, 14, 28 or day 0, 7, 14. The mice were maintained at an ambient room temperature, 40-60% humidity and a 14h:10h day/night cycle. Retro-orbital blood was drawn using heparinized micro capillary tubes (Fisher, Cat. No. 22362566) and collected in lithium heparin microtainers (Fisher, Cat. No. 13-680-62) at indicated time points.

Isolation of plasma and peripheral blood mononuclear cells (PBMCs) from blood

The collected blood was 1:1 diluted with 2% FBS and was added to 7ml of Lymphoprep[™] density gradient medium in SepMate-15 tubes (StemCell Technologies). The red blood cells, PBMCs and plasma were isolated from blood by centrifugation at 1200 x g for 20 min. After centrifugation, approximately 200 to 300 µl plasma was collected from the surface layer and the PBMCs in the remaining solution at the top

were poured to a new tube. The separated PBMCs were washed with 2% FBS and sample's mRNA was extracted using RNeasy Plus Mini Kit (Qiagen).

ELISA

Commercial MPXV antigens used in ELISA include E8L (AcroBiosystems, E8L-M52H3), M1R (Sino Biological, 40904-V07H), B6R (Sino Biological, 40902-V08H), A35R (Sino Biological, 40886-V08H), and A29L (Sino Biological, 40891-V08E). Recombinant antigens at 3 µg/ml in PBS were coated on the 384-well microplate (Fisher, Cat. No. 07-000-877) in cold room overnight. On next day, the plate was washed three time with PBST (0.05% Tween-20) on 50TS microplate washer (Fisher Scientific, NC0611021), and was blocked with 0.5% BSA in PBST at room temperature for one hour. Plasma was twofold serially diluted with PBS at a starting dilution of 1:500. The plasma diluent was added to the plate and incubated at room temperature for one hour. After washing with PBST five time, the plate was incubated with anti-mouse IgG (H+L) secondary antibody (Fisher, A16072) at room temperature for one hour. The secondary antibody with horse radish peroxidase was 1:2500 diluted in 0.5% BSA blocking buffer before adding to the microplate. The plate was washed five times with PBST and developed with tetramethylbenzidine substrate (Biolegend, 421101). After 20 min at room temperature, the reaction was stopped with 1M phosphoric acid and OD450 was measured by multimode microplate reader (PerkinElmer EnVision 2105, Envision Manager v1.13.3009.1401). The dilution-dependent area under curves (AUC) was calculated from AUC subtracted by the background AUC, which is the product of log dilution difference and end dilution OD450 (details in data summary excel file).

Functional T cell response assay

The PBMCs were separated by Lymphoprep™ and SepMate-15 as described above. To remove red blood cells, the collected PBMCs were resuspended in 1ml ACK lysis buffer (Gibco, A1049201) and kept at room temperature for 5min. After ACK lysis, the PBMCs were resuspended in 2% FBS PBS and cell density was counted by automated Corning cell counter (Corning™ 6749). Approximately 0.5 million PBMCs from each mouse were cultured in 96-well U bottom plate in 200 µl complete RPMI medium with 10% FBS, 50 µM 2-mercaptoethanol, 1 µg/ml LEAF™ Purified anti-mouse CD28 Antibody (Biolegend, 102116), Non-Essential Amino Acids (Gibco, 11140050), GlutaMAX™ (Gibco, 35050061), 1 mM Sodium pyruvate (Gibco, 11360070) and Penicillin-Streptomycin (Gibco, 15140122). eBioscience™ Cell Stimulation Cocktail (500X, Thermo Fisher 00-4970-93) was used to stimulate the positive control samples. Equal-mass mixture of Mpox protein antigens (seen in ELISA section) were added to experimental groups including negative

control group. Matching amount of DMSO (0.2%) was added to negative control samples for flow gating optimization. PBMCs were cultured for 14-16 hours. The supernatant was collected and secreted cytokines were quantified by mouse Th1/Th2 8plex LEGENDplex kit (Biolegend, Cat. No. 741054).

Cell line and virus culture

BS-C-1 kidney epithelial cells were cultured in Dulbecco's Modified Eagle Medium (DMEM) supplemented with 1% sodium pyruvate (NEAA) and 10% fetal bovine serum (FBS) at 37°C and 5% CO₂. SL-29 embryo chicken cells were cultured in Dulbecco's Modified Eagle's Medium (DMEM) supplemented with 1% sodium pyruvate (NEAA), 5% fetal bovine serum (FBS) and 5% tryptose phosphate broth at 37°C and 5% CO₂. HeLa cervical cancer cells were cultured in Dulbecco's Modified Eagle Medium (DMEM) supplemented with 1% sodium pyruvate (NEAA) and 10% fetal bovine serum (FBS) at 37°C and 5% CO₂. All cell lines tested negative for contamination with mycoplasma.

Cowpox Virus, Brighton Red was obtained from BEI Resources (#NR-88). Monkeypox virus (hMPXV/USA/MA001/2022), was obtained from BEI Resources (#NR- 58622), which was delivered as cell lysate. Vaccinia Virus was obtained from BEI Resources (#NR-53). Cowpox and Mpox viruses were cultured and expanded in BS-C-1 cells. Vaccinia virus was cultured in SL-29 cells and then expanded in HeLa cells. Fresh cultures were inoculated with the lysates as described above for viral expansion. Viral titers were measured by standard plaque assay using BS-C-1 cells or HeLa cells. Briefly, 300 µl of serial fold virus dilutions were used to infect cells in MEM supplemented NaHCO₃, 4% FBS 0.6% Avicel RC-581. Plaques were resolved at 4 days post-infection by fixing in 10% formaldehyde for 1h followed by 0.5% crystal violet in 20% ethanol staining. Plates were rinsed in water to plaques enumeration. Mpox experiments were performed in a biosafety level 3 laboratory with approval from the Yale Environmental Health and Safety office.

Neutralization assay

Mouse sera was heat treated for 30 min at 56°C, prior to infectious virus neutralization assay in order to remove complements and other potential neutralizing agents. Three-fold serially diluted sera, from 1:10 to 1:2430 were incubated with VACV, CPXV or Mpox virus, for 1 h at 37 °C. Mouse complement was added to the mixtures at a final concentration of 2%. The mixture was subsequently incubated with HeLa or BS-C-1 cells for 1h, for adsorption. Then, cells were overlaid with MEM supplemented with NaHCO₃, 4% FBS and 0.6% Avicel mixture. Plaques were resolved at 4 days post infection by fixing in 10% formaldehyde

for 1 h followed by staining in 0.5% crystal violet. All experiments were performed in parallel with baseline controls sera, in an established viral concentration to generate 60-120 plaques/well. Neutralization titers were calculated as area under curve (AUC) of titration curves.

Vaccinia virus challenge experiment

Age matched female BALB/c mice were used in the challenge experiments. Mice were intramuscularly injected with three doses of 5 µg MPXVac-097 or Mix-5 (total RNA mass) LNP mRNAs on day 0, 7 and 14. Mice were inoculated intranasally with Vaccinia Virus, Lederle-Chorioallantoic, 2×10^6 pfu/mouse. As a control group, mice were immunized subcutaneously with Vaccinia Virus, Lederle-Chorioallantoic, 2×10^5 pfu/100ul/mouse, 14 days prior challenge. Animals were monitored daily and viral infection was determined by survival, weight loss and disease signs. The percent of body weight change was normalized by the maximum body weight in the first three days post viral challenge. The following criteria were used to measure the clinical score of mice: 1, lethargy; 2, ruffled hair, hunched posture; 3, weight loss of $\geq 10\%$; 4, death. Experiments were conducted in compliance with protocols approved by the IACUC at Yale University.

Bulk TCR sequencing of PBMCs

Bulk TCR library was prepared using 200 ng mRNA extracted from PBMCs collected on day 0 (pre-vaccination) and day 20 (post boost) mice as described above. The SMARTer Mouse TCR a/b Profiling Kit (Takara, Cat. No. 634403) was used to amplify both TCR α and TCR β sequences. The purified amplicon concentration and purity was determined using D5000 high sensitivity tapes on TapeStation (Agilent). Equal amount of TCR amplicons from each sample was pooled and diluted with water to get a 2nM library. The pooled library was denatured, mixed with 5% PhiX and sequenced on MiSeq (Illumina) using MiSeq V3 2 x 300 cycle kit (Illumina).

VDJ sequencing data analysis

The bulk VDJ sequencing data was pre-processed on MiSeq local run manager to trim adaptors and separate reads based on sample index. The reads with an average quality score less than 30 were removed from downstream analysis. Clonotypes were called using MiXCR v2.1.5 with the recommended settings for 5' RACE (RNA alignment to V gene transcripts with P region). The output was further processed with Immunarch v0.6.6 R package for statistical analyses using standard analysis pipelines. The initial samples were n = 5 independent mouse samples, assessed pre-vaccination and post-boost (labeled D0 and D20,

respectively) in paired analyses. Samples were assessed for outliers by a multi-step process, (1) comparing the repertoire overlap (amino acid sequence and V gene) between samples using the Morisita method, separately for TRA AND TRB, (2) performing principal components analysis on combined TRA and TRB overlap information (Morisita indices), (3) determining the optimal PCs for subsequent analysis (details below), (4) calculating Mahalanobis sample distances using the optimal number of PCs, and (5) calculating p values using a chi-squared distribution (2 degrees of freedom for 2 PCs) and correcting for multiple testing using the FDR method (Supplementary information, Fig. S12). The optimal number of PCs was chosen as two using the elbow plot method, and the choice was supported by PC scatter plots that demonstrated that PC1 best explained outlier samples, PC2 best explained the treatment differences, while Pearson correlation analyses of PC1 and PC2 demonstrated the best treatment specific correlation. Estimates were calculated using the “true diversity” method, based on amino acid sequences (Fig. 1f). The filtering parameter excluded two TCR libraries, one from each group (D0 or D20), and the final TCR analysis consists of four samples from each group (n = 4 each). Fig. 1f-1g analyses were performed with n = 4 paired pre-vaccination and post-boost samples.

Mouse necropsy, histology, semiquantitative pathologic analysis

The 8-week-old female C57BL/6NCr mice were randomized into MPXVac-097 vaccination group or no treatment group. Six days after final immunization, mice were submitted blind to experimental treatment for a complete mouse necropsy to the Comparative Pathology Research Core (Department of Comparative Medicine, Yale University school of Medicine), a plasma chemistry and a complete blood count (Antech Diagnostic Laboratory, ADL, NY) by routine methods. Briefly, mice were euthanized by CO₂ narcosis followed by exsanguination by terminal cardiac puncture. The blood was placed in an EDTA tube, refrigerated and submitted ADL. The soft tissues (heart, lung, liver spleen, kidneys, adrenal glands, gastrointestinal tract, genitourinary tract, and skin) were immersion-fixed in neutral buffered 10% formalin (Fisher Scientific). The rear limb, sternum, and the skull with brain were immersion-fixed in Bouin’s solution (Ricca Chemical Company, Arlington, TX). Tissues were trimmed, cassetted, processed, embedded in paraffin, and sectioned at 5 microns and stained with hematoxylin and eosin by routine methods (Yale Mouse Research Pathology, Section of Comparative Medicine, Yale University School of Medicine).

Tissues were examined blind to experimental group by routine light microscopy for pathologic changes and using an Olympus BX43F-1-3 Microscope. Digital light microscopic images were taken using an

Olympus DP28 1" 8.9MP color camera and CellSens Standard Version 4.1 imaging software (Olympus Scientific Solutions Americas Corp DBA EVIDENT SCIENTIFIC, Waltham MA). The digital images were optimized using Adobe Photoshop 23.0 (Adobe Corporation, USA). The liver microscopic findings were further characterized and scored for semiquantitative analysis modified from prior published methods^{25, 26} using standard pathologic nomenclature for the presence of single cell necrosis, extramedullary hematopoiesis, hepatitis, bile duct/ule hyperplasia and the presence of periductular lymphocytes/plasma cells using the following scale/score: within normal limits 0, scant 0.24, < min 0.5, minimal 1, mild 2, moderate, 3, marked 4, severe 5.

Statistics and Reproducibility

Standard statistical methods were applied to experimental data. The statistical methods are described in here, figure legends and/or supplementary Excel tables. Data on dot-bar plots are shown as mean \pm s.e.m. with individual data points in plots. Two-way ANOVA with Tukey's or Sidak's multiple comparisons test was used to assess statistical significance for grouped datasets. Statistics of Figure 1: **c**, Ordinary One-way ANOVA with Dunnett multiple comparison test; **d-e**, two-way ANOVA with Turkey's multiple comparison test. **f**, Kolmogorov-Smirnov test; **h**, one-way ANOVA with Dunnett's multiple comparison test; **i**, two-way ANOVA with Sidak's multiple comparison test; **j**, unpaired parametric t test. Additional statistical methods information of supplementary figures can be found in data summary excel file. Level of significance: * $p < 0.05$, ** $p < 0.01$, *** $p < 0.001$, **** $p < 0.0001$, and n.s., not significant. Non-significant comparisons are not shown, unless otherwise noted as n.s., not significant. Sample number is designated as n from biologically independent samples. Prism (version 9.3.2, GraphPad Software Inc.) and RStudio (version 1.3.959, RStudio software) were used for these analyses. Additional information can be found in the supplementary excel tables.

Schematic illustrations

Schematic illustrations were created with Affinity Designer or BioRender.

References

- 1 De Baetselier, I. et al. *Nat Med* (2022).
- 2 CDC. Interim Clinical Considerations for Use of JYNNEOS and ACAM2000 Vaccines during the 2022 U.S. Monkeypox Outbreak. Available from: <https://www.cdc.gov/poxvirus/monkeypox/considerations-for-monkeypox-vaccination.html>.
- 3 Rao, A. K. et al. *MMWR Morb Mortal Wkly Rep* **71**, 734-742 (2022).
- 4 Lum, F. M. et al. *Nat Rev Immunol* (2022).
- 5 Pittman, P. R. et al. *N Engl J Med* **381**, 1897-1908 (2019).
- 6 Hatch, G. J. et al. *J Virol* **87**, 7805-7815 (2013).
- 7 Kupferschmidt, K. *Science* **377**, 696-697 (2022).
- 8 Fang, Z. et al. *Nat Commun* **13**, 3250 (2022).
- 9 Fang, Z. et al. *Cell Discov* **8**, 108 (2022).
- 10 Baden, L. R. et al. *N Engl J Med* **384**, 403-416 (2021).
- 11 Davies, D. H. et al. *Proc Natl Acad Sci U S A* **102**, 547-552 (2005).
- 12 Meyer, H. et al. *J Gen Virol* **72** (Pt 5), 1031-1038 (1991).
- 13 Gong, Q. et al. *Viol Sin* **37**, 477-482 (2022).
- 14 Matho, M. H. et al. *J Virol* **86**, 8050-8058 (2012).
- 15 Davies, D. H. et al. *J Virol* **79**, 11724-11733 (2005).
- 16 Kaefer, T. et al. *J Virol* **88**, 11339-11355 (2014).
- 17 Matho, M. H. et al. *PLoS Pathog* **11**, e1005148 (2015).
- 18 Engelstad, M. et al. *Virology* **188**, 801-810 (1992).
- 19 Sakhatsky, P. et al. *Virology* **355**, 164-174 (2006).
- 20 Isidro, J. et al. *Nat Med* **28**, 1569-1572 (2022).
- 21 Belongia, E. A. et al. *Clin Med Res* **1**, 87-92 (2003).
- 22 Nalca, A. et al. *Drug Des Devel Ther* **4**, 71-79 (2010).
- 23 Gilchuk, I. et al. *Cell* **167**, 684-694 e689 (2016).
- 24 Gigante, C. M., et al. *bioRxiv* (2022).
- 25 Montgomery, R. R. et al. *Infect Immun* **75**, 613-620 (2007).
- 26 Bandi, P. et al. *Antimicrob Agents Chemother* **54**, 749-756 (2010).

Reporting summary

Statistics

For all statistical analyses, we confirmed that the items mentioned in NPG reporting summary are present in the figure legend, table legend, main text, or Methods section.

Standard statistical analysis

All statistical methods are described in figure legends, methods and/or supplementary Excel tables. Source data and statistics were provided in a supplemental excel table.

Software and code

Data collection

Default softwares in the data collection instruments including Attune focusing cytometer (Attune NxT Software v3.1) and PerkinElmer EnVision 2105 microplate reader (Envision Manager v1.13.3009.1401) were used to collect data.

Data analysis

Data analysis were performed using Prism (version 9.3.1, GraphPad Software Inc.) for small scale data. NGS data were analyzed with custom codes.

Data and resource availability

All data including source data and statistics in this study are included in main or supplementary files. NGS data has been deposited to GEO (GSE225183). Other materials and custom codes are available via reasonable requests to the corresponding authors.

Code availability

Custom codes are available either through public repositories, or via reasonable requests to the corresponding author to the academic community.

Life sciences study design

Sample size determination

For most cases, each group has five biologically independent samples unless otherwise noted. Details on sample size for each experiment were indicated in methods and figure legends. Sample size was determined according to the lab's prior work or similar studies in the field.

Data exclusions

Five independent mice were initially used for TCR-seq library prep. In two TCR libraries, one paired sample No. 4 from two groups (D0 or D20) did not pass QC and thus were excluded from subsequent analysis. This is noted in methods section and figure legend.

No other data were excluded.

Replication

Biological replicates of mouse samples were done in each experiment.

Randomization

Mice were randomly allocated into experimental or control groups.

Blinding

The ELISA, confocal and flow experiments were not blinded. Neutralization, in vivo mouse challenge and toxicity experiments were blinded. NGS data were initially processed with blinded barcoded metadata.

Reporting for specific materials, systems and methods

Antibodies used

1. HRP-conjugated anti-mouse IgG (H+L) antibody (Fisher, Cat. No. A16072, 1:2500 dilution)
2. PE-conjugated anti-mouse IgG (H+L) antibody (Fisher, Cat. No. P-852, 1:100 dilution)
3. PE-conjugated anti-flag antibody (Biolegend, Cat. No. 637310, 1:50 or 1:100 dilution)

Antibody validation

Commercial antibodies were validated by the vendors, and re-validated in house as appropriate through antigen-specific experiments. Commercial antibody info and validation info where applicable:

1. HRP-conjugated anti-mouse IgG (H+L) antibody (Fisher, Cat. No. A16072, 1:2500 dilution): [Goat anti-Mouse IgG \(H+L\) Cross-Adsorbed, HRP \(A16072\) \(thermofisher.com\)](#)

2. PE-conjugated anti-mouse IgG (H+L) antibody (Fisher, Cat. No. P-852, 1:100 dilution): [Goat anti-Mouse IgG \(H+L\) Cross-Adsorbed, PE \(P-852\) \(thermofisher.com\)](#)

3. PE-conjugated anti-flag antibody: <https://www.biolegend.com/en-us/search-results/pe-anti-dykdjdk-tag-antibody-9383?GroupID=GROUP26>

Eukaryotic cell lines

Commercial cell line HEK293T was originally acquired from ATCC (CRL-3216).

Authentication

Cell lines were authenticated by original vendors, and re-validated in lab as appropriate by morphology.

Mycoplasma contamination

All the cell lines used here tested negative for mycoplasma contamination.

Commonly misidentified lines (See ICLAC register)

No misidentified cell lines were used in the study.

Animals and other organisms

Laboratory animals

C57BL/6Ncr (B6) mice, female 8-10 week mice purchased from Charles River.

Wild animals

N/A

Field-collected samples

N/A

Ethics oversight

The work described in this study is performed under relevant approved protocols (IACUC, rDNA/EHS) in place.

Flow Cytometry

Plots

Confirm the checkboxes of requirements.

Methodology**Sample preparation**

Various sample prep details are provided in the Methods section

Instrument

Flow cytometry data were collected on Attune focusing cytometer (Attune NxT Software v3.1)

Software

FlowJo v.10.7.1 was used for flow cytometry data analysis.

Cell population abundance

N/A

Gating strategy

Cells were gated by FSC/SSC plot. To distinguish between positive and negative boundaries of the stained cells, negative control samples were analyzed and utilized as background.

Gating example figure

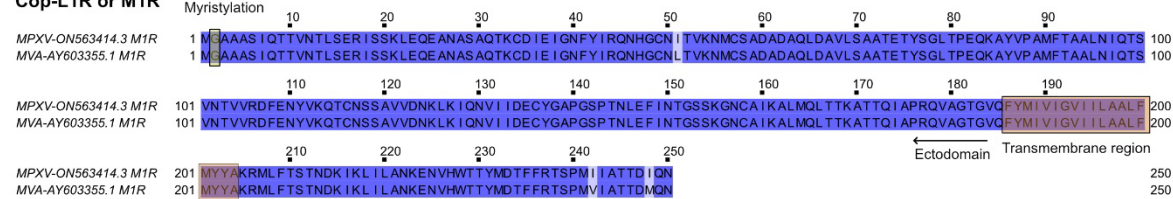
We confirm that a figure exemplifying the gating strategy is provided in the Supplementary Information.

Supplementary figures and legends

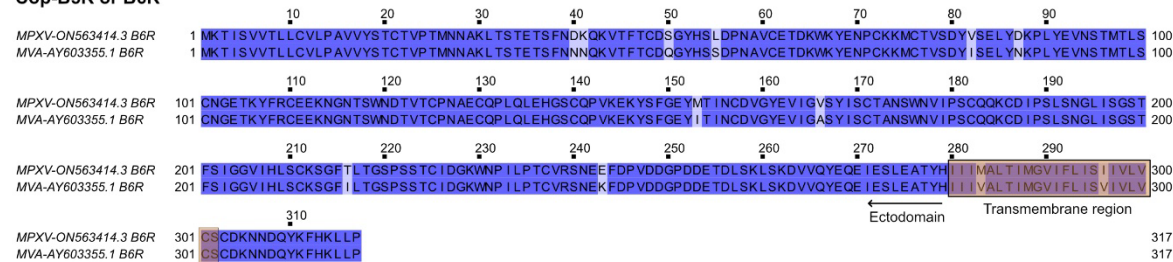
Cop-D8L or E8L



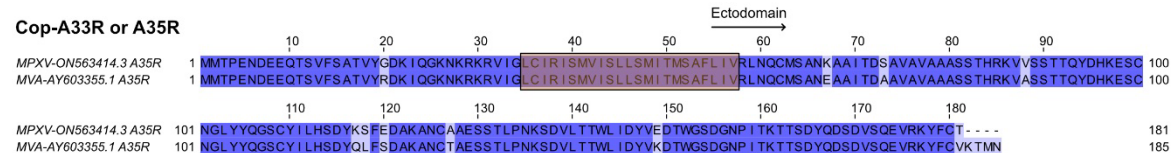
Cop-L1R or M1R



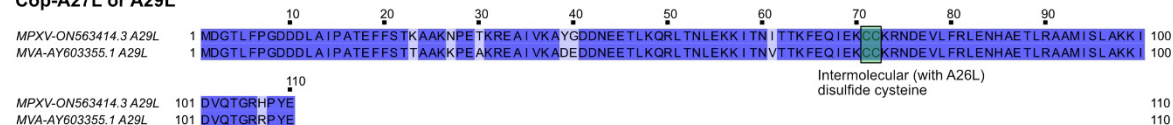
Cop-B5R or B6R



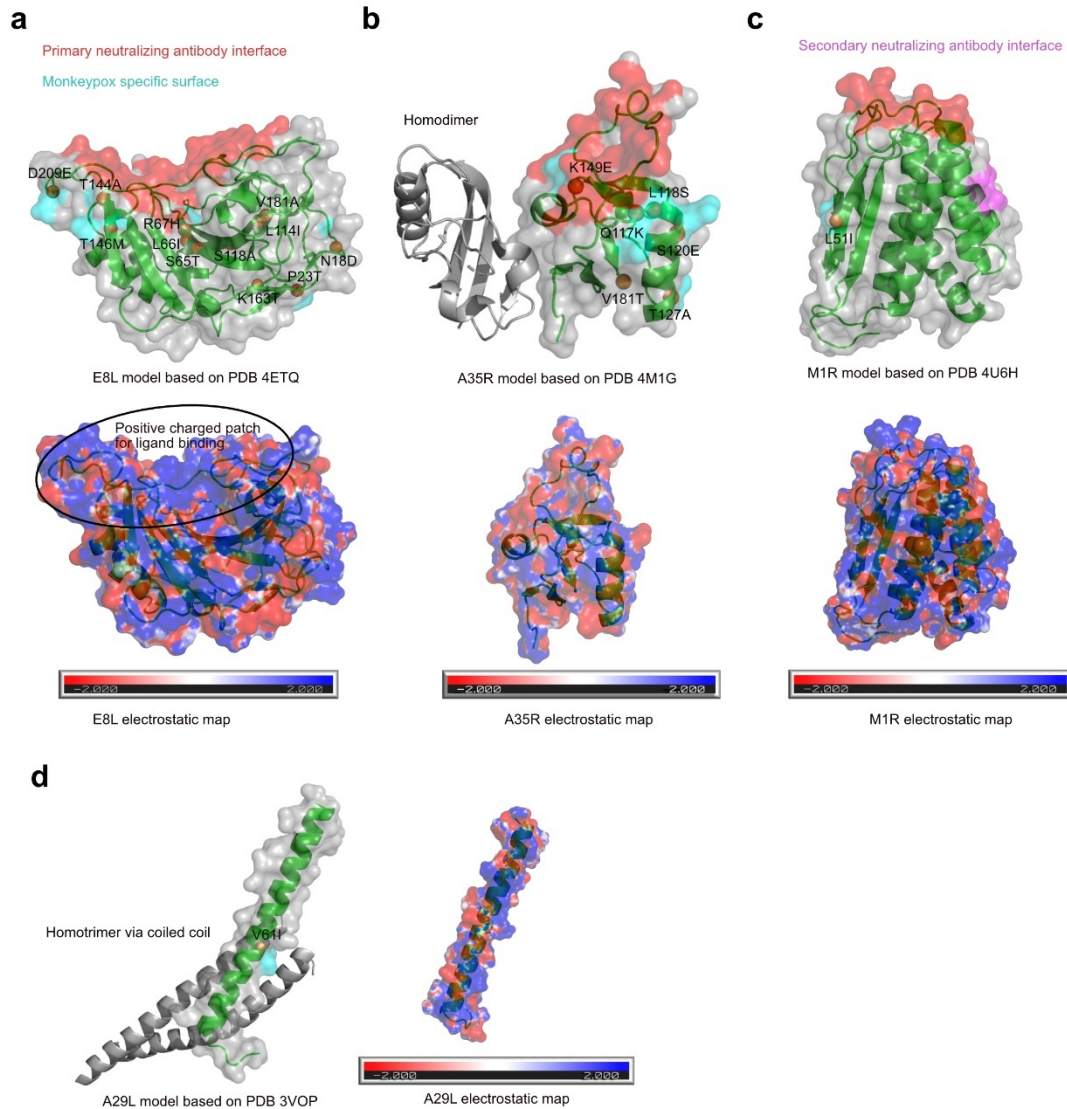
Cop-A33R or A35R



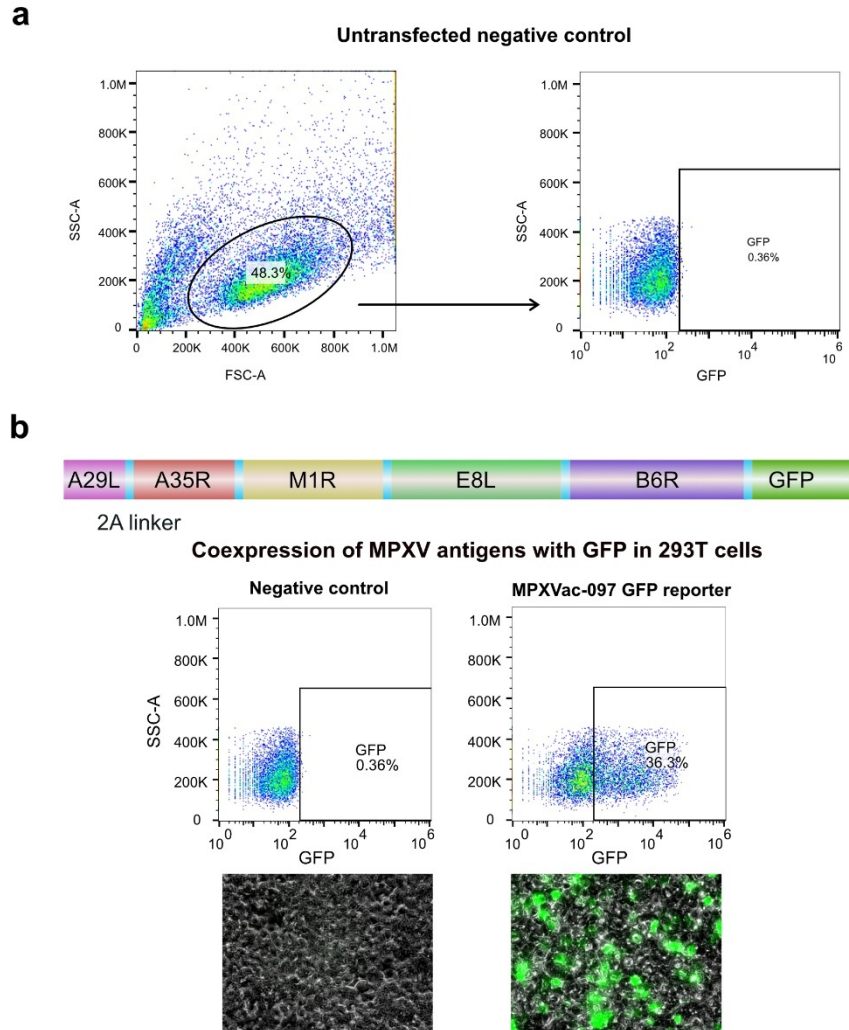
Cop-A27L or A29L



Supplementary information, Fig. S1. Sequence alignment of five antigen homologs from monkeypox (GenBank ON563414.3) and MVA (GenBank AY603355.1). Transmembrane domains and ectodomains of each antigen are indicated on the sequences.



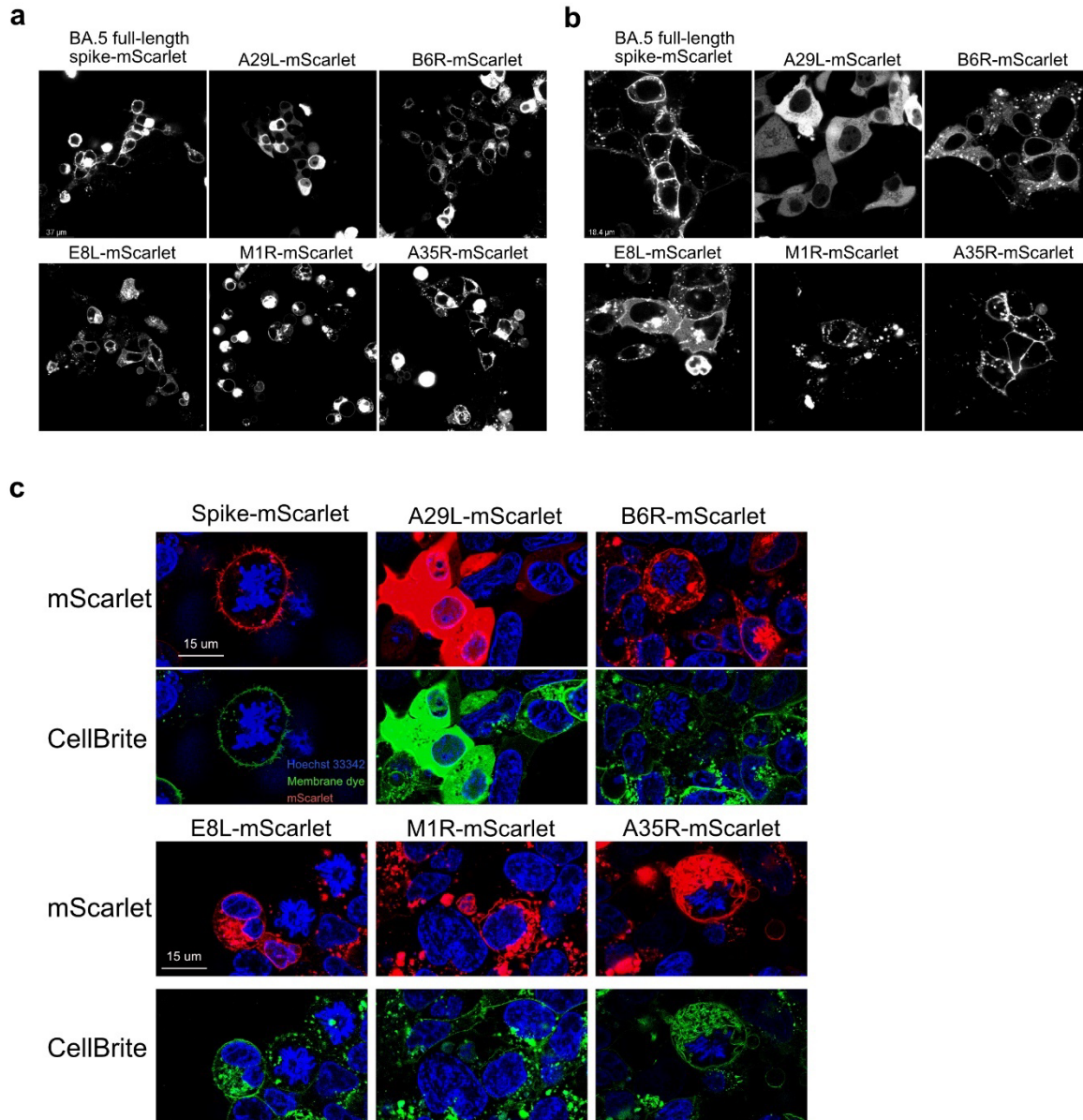
Supplementary information, Fig. S2. Calculated electrostatic map on homolog structures of four monkeypox virus antigens (a-d). The antigen sequence differences between monkeypox and MVA are displayed on corresponding homology structural models. The monkeypox specific surface that differs from MVA is colored in cyan. The surface electrostatic map was generated using CHARMM-GUI server ([CHARMM-GUI](http://charmm-gui.org)) and SWISS homology models ([SWISS-MODEL \(expasy.org\)](http://swiss-model.expasy.org)).



Supplementary information, Fig. S3. Expression of GFP appended to the C term of MPXVac-097 suggests successful transcription and translation of genes in MPXVac-097.

a, Untransfected 293T cells as negative controls to select gating strategy used in flow cytometry.

b, Co-expression of five monkeypox antigens and GFP in 293T cells. The GFP positive cells with expression of five monkeypox antigens are identified by flow cytometry and fluorescence microscope.

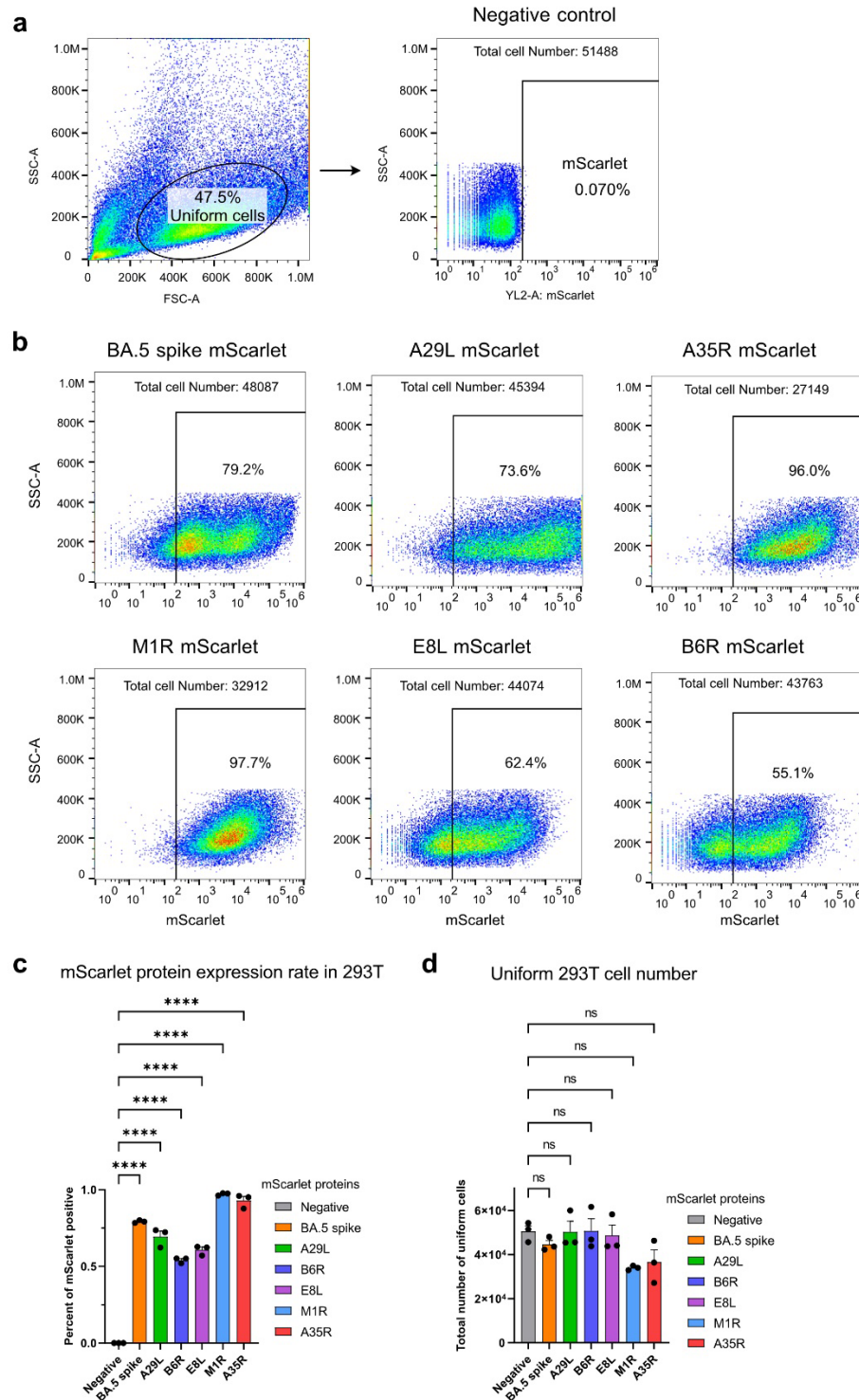


Supplementary information, Fig. S4. mScarlet tagged monkeypox antigen's localization in 293T cells visualized by confocal microscopy.

a-b, Cellular localization of individual monkey antigens with C-term mScarlet. All micrographs are at the same magnification and supplementary Fig. 4a is half of magnification of supplementary Fig. 4b.

c, 293T live cells expressing mScarlet (red) tagged monkeypox antigens were co-stained with CellBrite-Green membrane dye (green) and Hoechst 33342 (blue) to identify different cellular compartments under confocal microscopy. Raw images were deconvoluted to enhance resolution and contrast.

The scale bar is shown in the first micrograph.



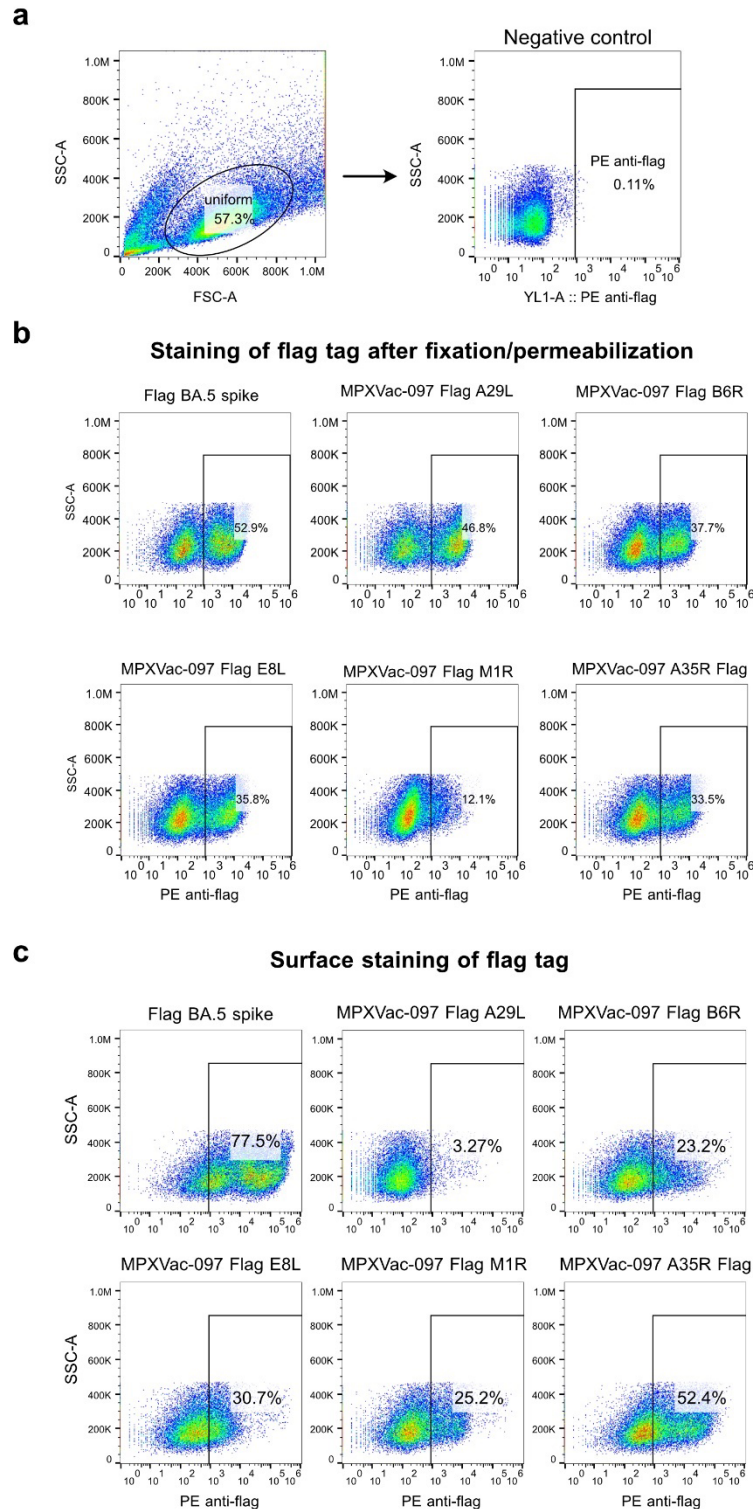
Supplementary information, Fig. S5. mScarlet tagged monkeypox antigen expression level in 293T cells as determined by flow cytometry.

a, Representative gating strategy in negative control cells. The total number of uniform cells is displayed in the right panel.

b, the percent of mScarlet positive populations in cells expressing monkeypox antigens or SARS-CoV-2 spike is shown in each graph. Each group has three biological replicates (n=3)

c, mScarlet positive rates of each antigen expression group are summarized in the bar graph.

d, the number of uniform cells collected from 40ul cell suspension was compared among different antigen expression groups.

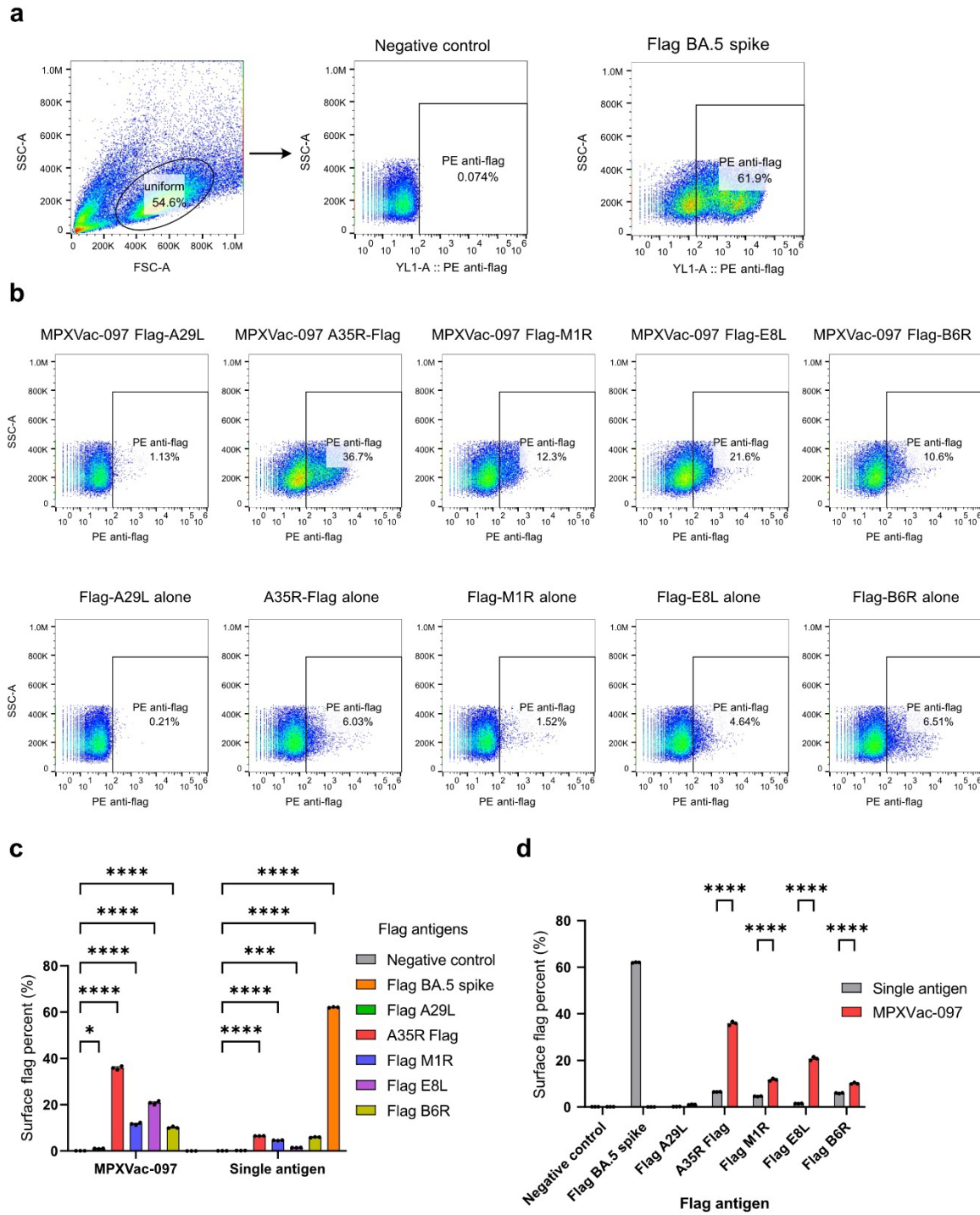


Supplementary information, Fig. S6. Staining of surface or whole-cell flag-tagged monkeypox antigens in MPXVac-097 expressed in 293T cells.

a, Gating strategy to define uniform cells and flag positive population based on negative control cells

b-c, Representative flow cytometry micrographs of whole-cell-stained (b) or surface-stained (c) 293T cells co-expressing monkeypox antigens (2.5 µg plasmid per 12 well) in tandem tagged by flag at ectodomain end in each gene position of MPXVac-097.

Flag was added after the signal peptide if any, and its N-term or C-term position was indicated by its appearance before or after the antigen name, respectively. These flow plots correspond to data in Fig. 1c.



Supplementary information, Fig. S7. Surface staining of flag tagged monkeypox antigens co-expressed in MPXVac-097 in 293T cells or individually expressed in 293T cells.

a, Representative plots to show gating strategy that defines uniform cells (left) and flag positive (mid and right) populations in negative control cells and cells expressing flag BA.5 spike.

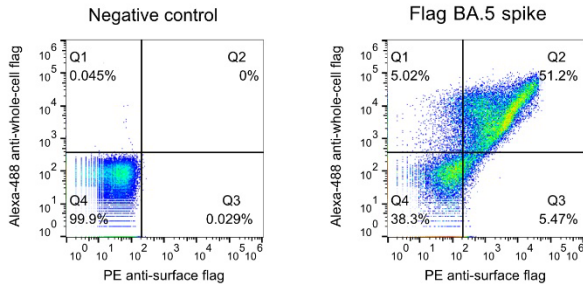
b, Representative plots to compare surface flag positive rates of monkeypox antigens co-expressed in MPXVac-097 in 293T cells (only one indicated position is flag tagged) vs. those individually expressed in 293T cells (1.25ug plasmid per 12 well).

c, Bar plots comparing the percentages of surface flag positive cells expressing flag Mpox antigens alone (right) or in tandem in MPXVac-097 (left).

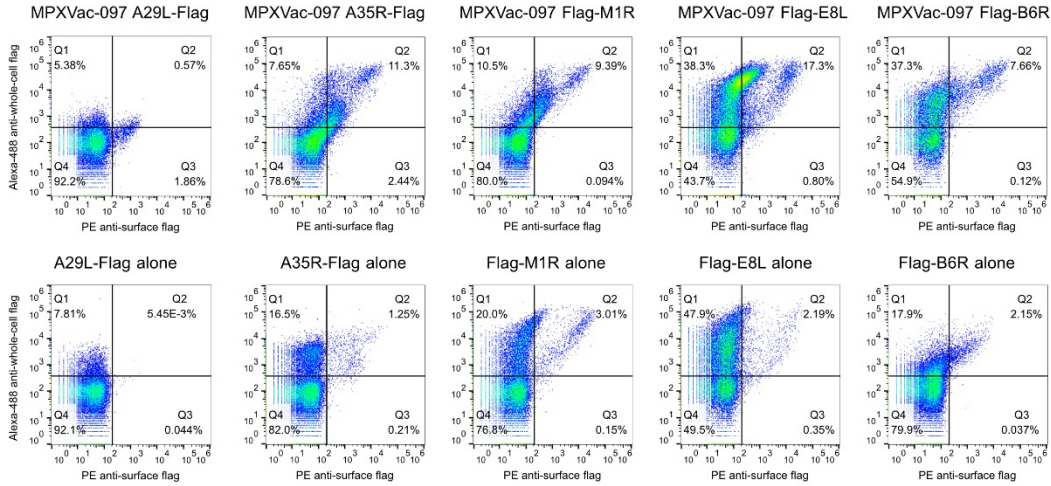
d, Bar plots comparing the percentages of surface flag positive cells expressing flag Mpox antigens alone (grey) or in tandem in MPXVac-097 (red).

Each group has three biological replicates. Data on bar plots are shown as mean \pm s.e.m. with individual data points in plots.

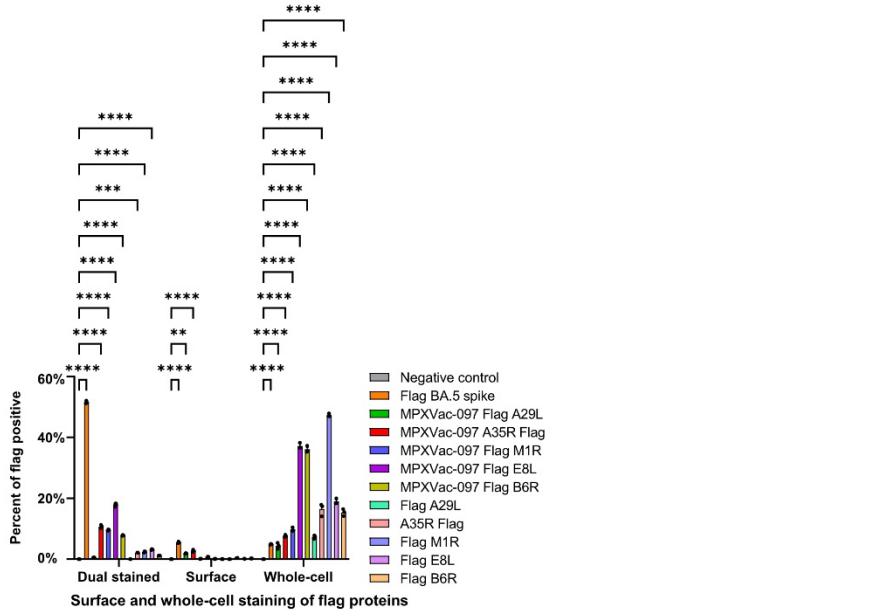
a



b



c



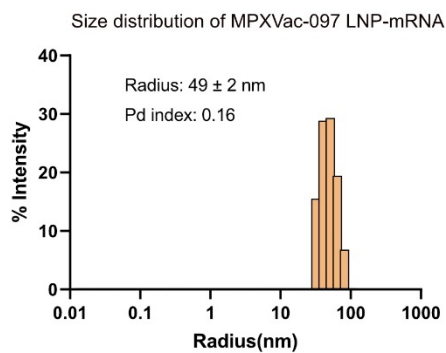
Supplementary information, Fig. S8. Dual staining of surface and whole-cell flag-tagged monkeypox antigens in MPXVac-097 as compared to those individually expressed in 293T cells.

a, Gating strategy that defines surface flag/PE positive (x axis), whole-cell flag/Alexa-488 positive (y axis) and dual positive populations in negative control cells and cells expressing flag BA.5 spike.

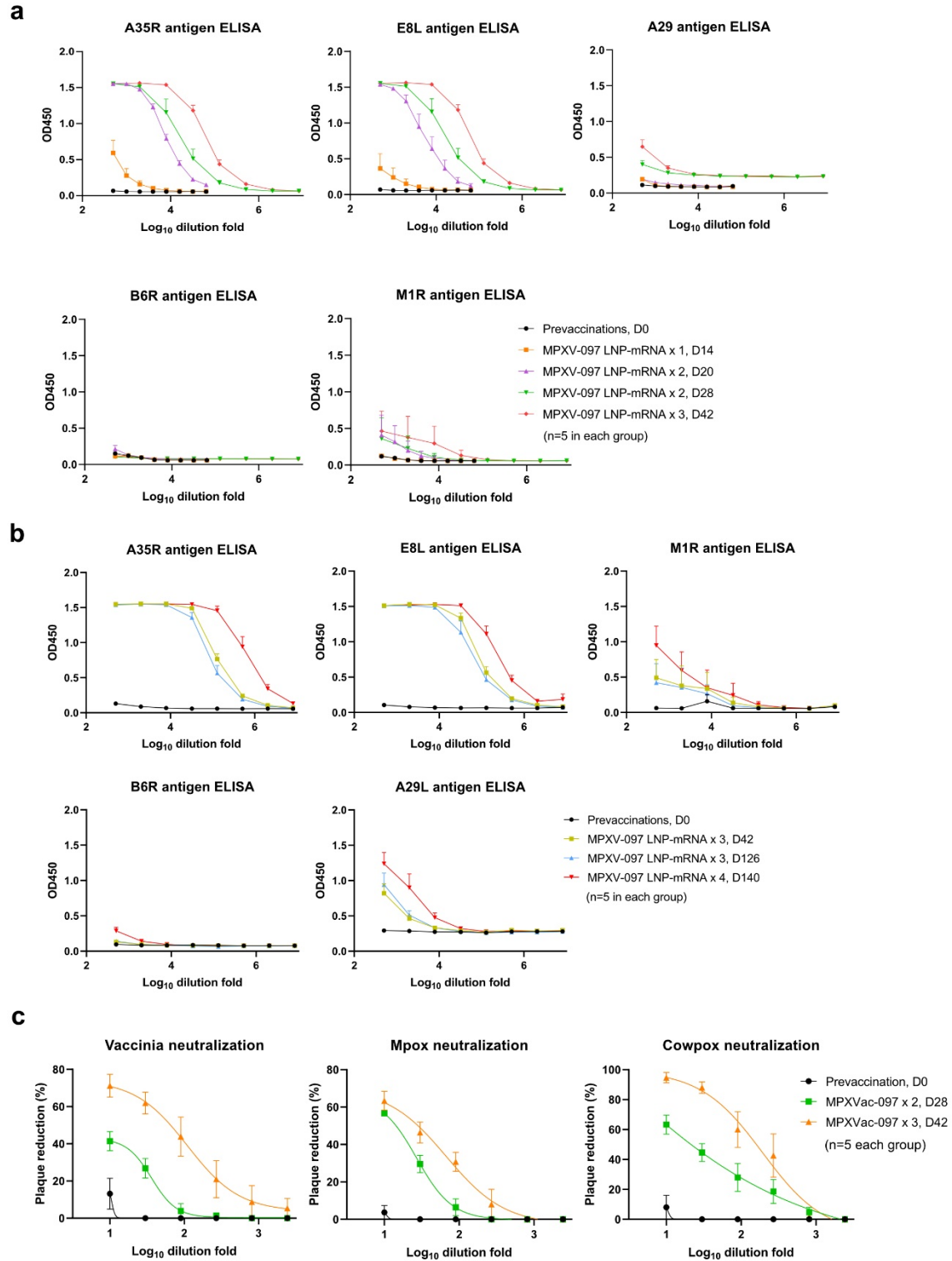
b, Representative plots to simultaneously compare surface and whole-cell flag positive rates of monkeypox antigens co-expressed in MPXVac-097 (only one position is tagged at a time) vs. those single expressed in 293T cells (1.25ug plasmid per 12 well).

c, bar graph summarizing surface and total flag positive percentage in 293T cells. Each group has three biological replicates. Data on bar plots are shown as mean \pm s.e.m. with individual data points in plots.

a



Supplementary information, Fig. S9. Size distribution of MPXVac-097 LNP-mRNA as determined by dynamic light scattering.



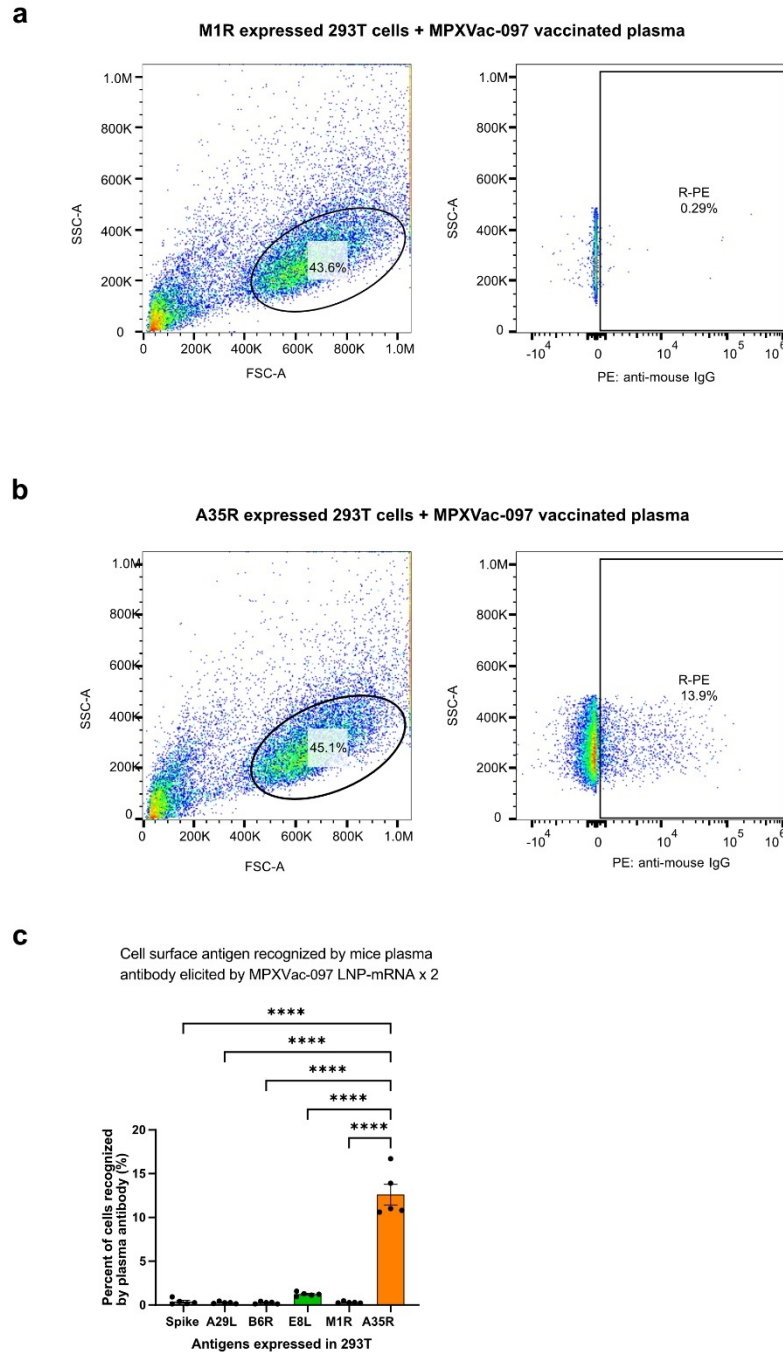
Supplementary information, Fig. S10. Titration curves of ELISA and plaque reduction neutralization test (PRNT).

a, ELISA titration curves showing binding response (OD450 on y axis) over serial dilution points of plasma samples (\log_{10} transformed dilution factor on x axis) collected from mice vaccinated with zero, one, two or three doses of MPXVac-097 LNP-mRNA on day 0, 14, 20, 28 and 42.

b, Titration curves showing binding response (OD450 on y axis) to each monkeypox antigen over serial dilution points of plasma samples (\log_{10} transformed dilution factor on x axis) collected from mice with and without vaccination of MPXVac-097 LNP-mRNAs on day 0, 42, 126 and 140. The area under curve (AUC) of these titration curves were used to calculate antibody titers of Fig. 1d.

c, PRNT titration curves showing percent of plaque reduction (y axis) over serial dilution of plasma samples (\log_{10} transformed dilution factor on x axis) collected from mice vaccinated with zero, two or three doses of MPXVac-097 on day 0, 28 and 42.

Vaccination schedule is shown in Fig. 1d. Each group's sample number is 5.



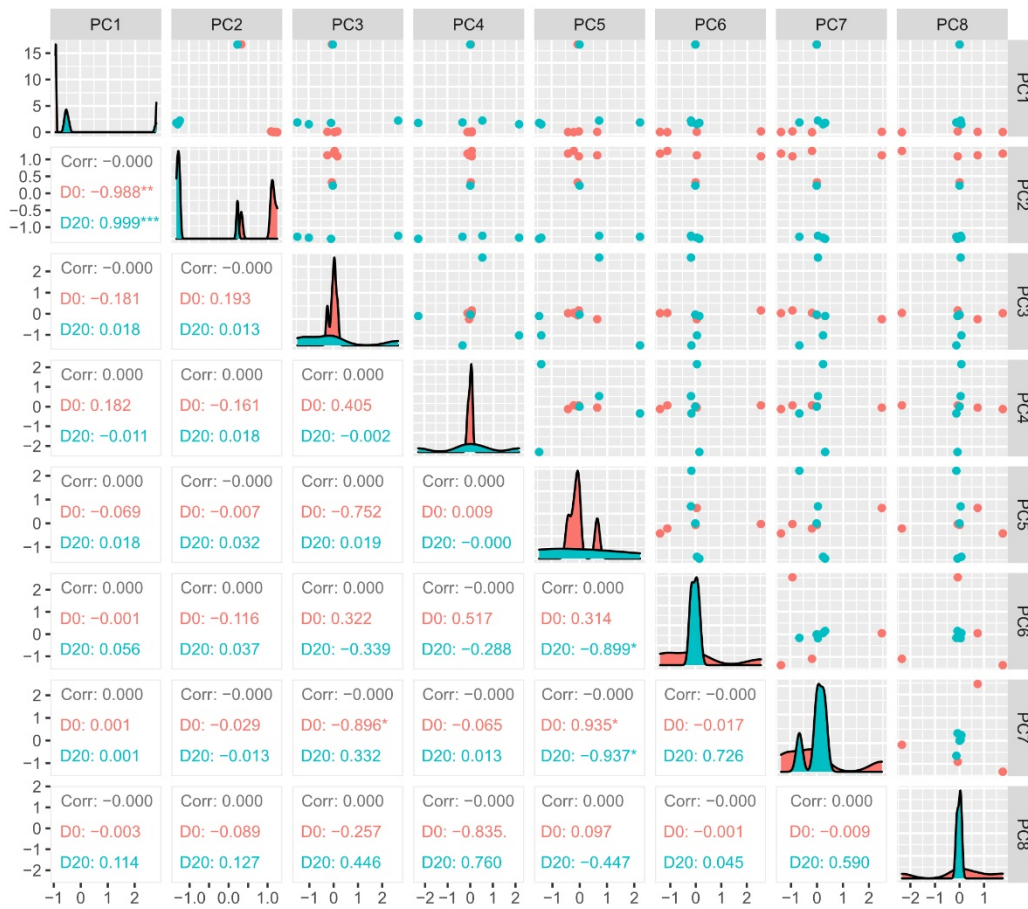
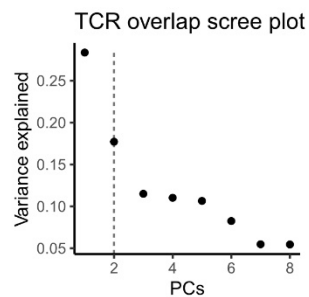
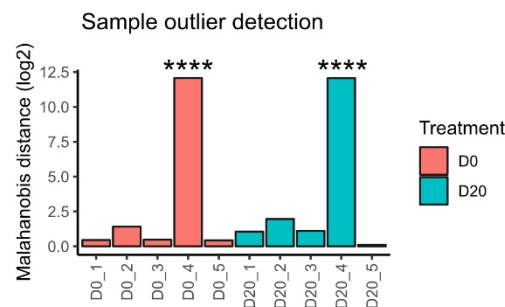
Supplementary information, Fig. S11. Flow cytometry to identify mice antibody bound 293T cells expressing monkeypox antigens.

Plasma samples were collected on day 20 from mice immunized with two doses of MPXV LNP-mRNAs and the primary mice antibody bound to the cells was recognized by anti-mouse IgG secondary antibody with PE fluorophore.

a-b, gating strategy of flow cytometry for cells expressing M1R (a) or A35R (b) antigens.

c, Monkeypox antigens expressed on 293T cell surface were recognized by plasma antibody produced from mice on day 20. SARS-CoV-2 spike expressing cells were served as a negative control.

Data on bar plots are shown as mean \pm s.e.m. with individual data points in plots.

a**PCA of repertoire overlap****b****c**

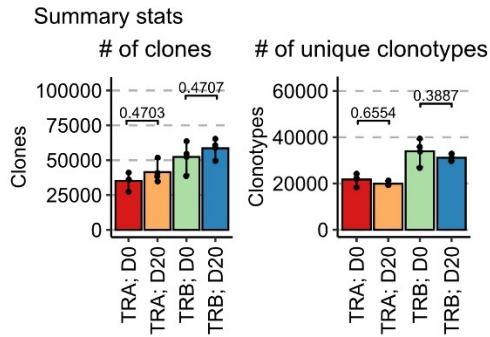
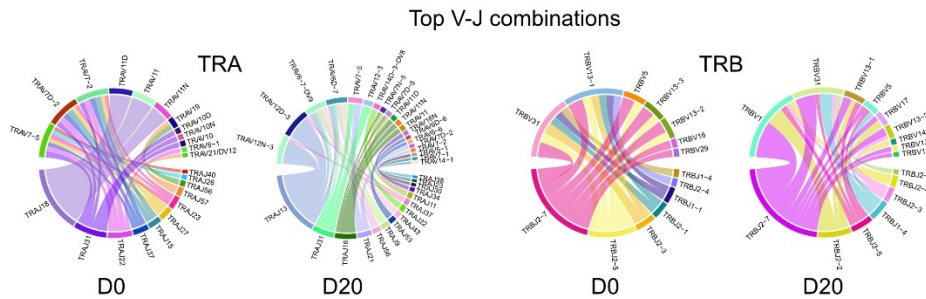
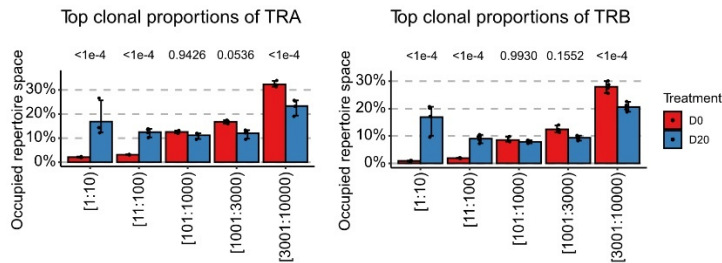
Supplementary information, Fig. S12. Quality control and sample filtering of TCR sequencing in pre-vaccinated and MPXVac-097 post-boosted mice.

a, Plots comparing the first eight components from the principal components analysis (PCA) of TCR repertoire overlap between samples. TCR repertoire overlap (amino acid sequence with variable region gene) was assessed by Morisita index score for TRA and TRB separately, and PCA was performed with pooled index scores. Plots in the upper-right triangle compare PCs, while the panels of the bottom-left

triangle show Pearson correlation rho for the corresponding upper-right panel. Correlation rho are provided for total, pre-vaccination (D0), and post-boost (D20) in black, red, and blue, respectively.

b, Scree plot of the variance explained by each PC from the PCA of TCR repertoire overlap between samples. First two PCs were chosen for further analysis based on the elbow plot method.

c, Bar plot of the sample differences, using Mahalanobis distance calculated from the first two PCs. Statistical analyses were performed by chi-squared test for each sample, and results were FDR-corrected for multiple testing. Statistical significance labels: * $p < 0.05$; ** $p < 0.01$; *** $p < 0.001$; **** $p < 0.0001$. Non-significant comparisons are not shown.

a**b****c**

Supplementary information, Fig. S13. TCR gene repertoire analyses in pre-vaccinated and MPXVac-097 post-boosted mice.

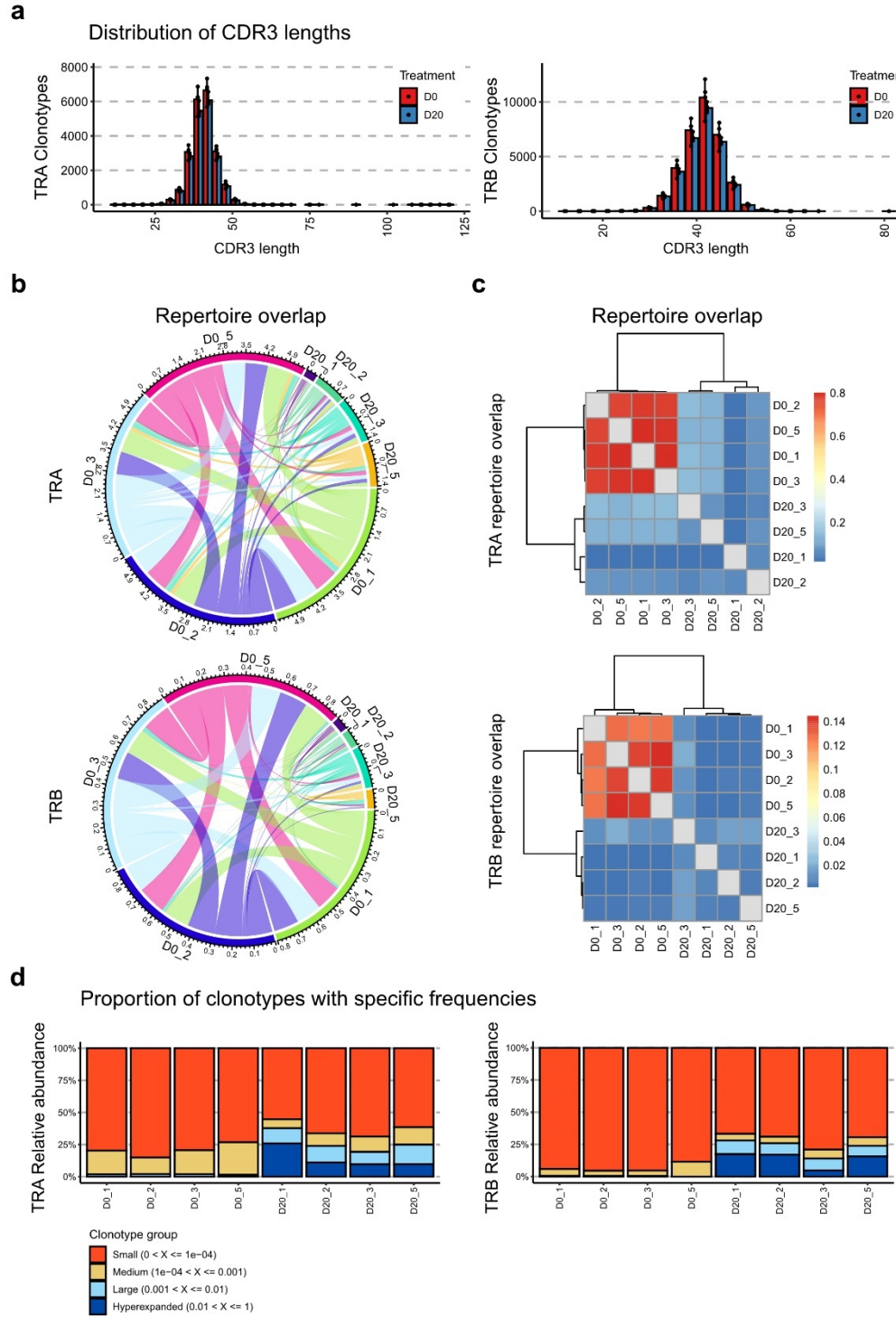
a, Bar plots for the number of clones and unique clonotypes detected between pre-vaccination (D0) and MPXV post-boost (D20) mice.

b, Circos plots of the top 20 TRA and TRB V-J gene combinations for pre-vaccination (D0) and post-boost (D20) of two-dose MPXVac-097 vaccinated mice. Replicate-pooled count data are presented in each plot.

c, Bar plots of the relative distribution of TCR clones between different ranges of top clonotypes. The data are presented with the index range of the most abundant clonotypes on the x axis and the percent of total repertoire on the y axis.

Statistics: **a** and **c**, two-way ANOVA with Sidak's multiple comparison test.

All analyses were performed with $n = 4$ paired pre-vaccination and post-boost samples. Data on bar plots are shown as mean \pm s.e.m. with individual data points in plots.



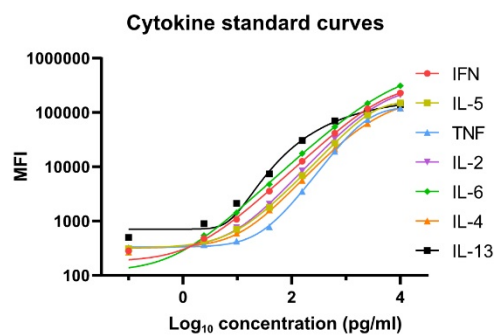
Supplementary information, Fig. S14. Summary statistics of TCR sequencing in pre-vaccinated and MPXV post-boosted mice.

a, Histograms of the CDR3 amino acid lengths for TRA and TRB clonotypes between pre-vaccination (D0) and post-boost (D20) two-dose MPXVac-097 vaccinated mice.

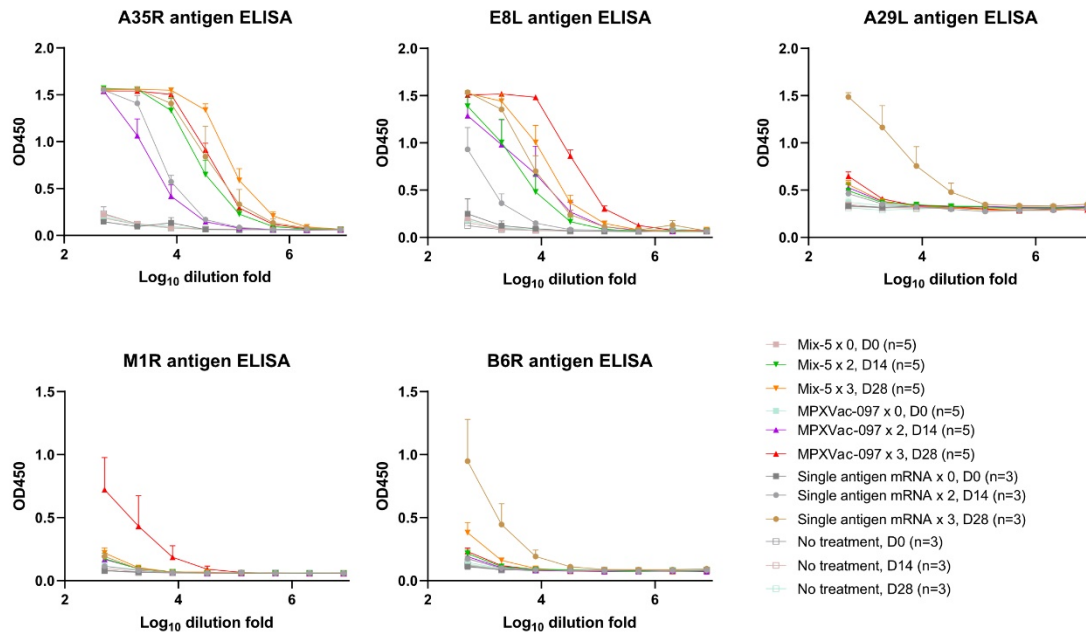
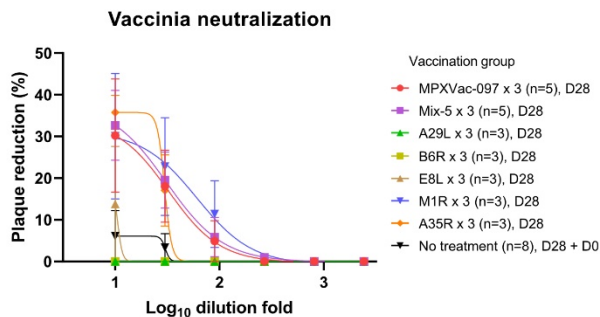
b-c, Circos, and bar plots (**b**, and **c**, respectively) of the TRA and TRB repertoire overlap between pre-vaccination (D0) and MPXV post-boost (D20) mice. Repertoire comparisons were performed using the Morisita method.

d, Stacked bar plots of the relative abundances of clones between different ranges of clonotype frequencies. The data are presented with the index range of the most abundant clonotypes on the x axis and the percent of total repertoire on the y axis.

a



Supplementary information, Fig. S15. Standard curves to quantify cytokine concentrations using LEGENDPlex kit.

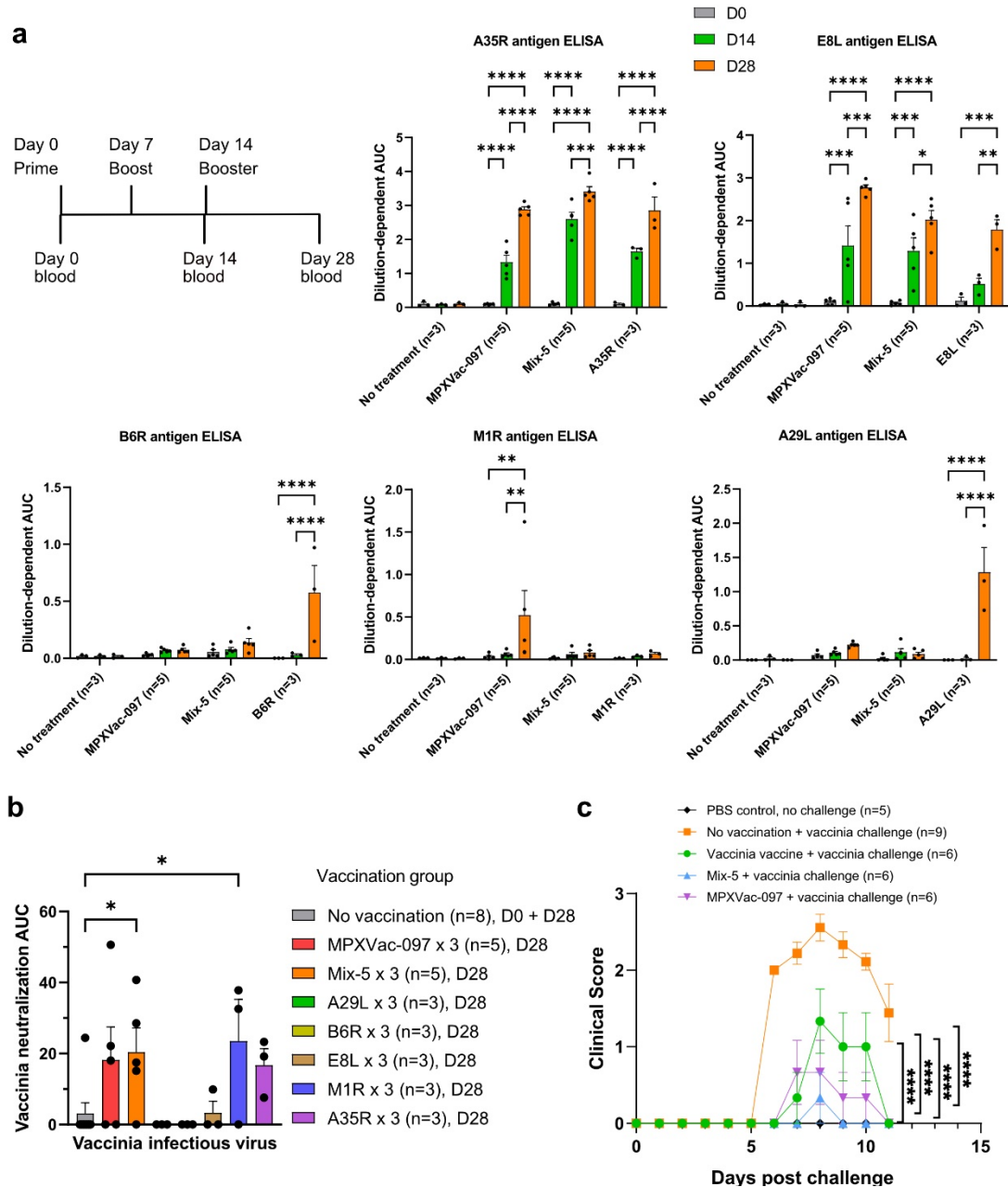
a**b**

Supplementary information, Fig. S16. Immunogenicity comparison of MPXVac-097 with Mix-5 and single antigen LNP-mRNAs in mice. ELISA and neutralization titration curves

a, Titration curves showing binding response (OD450 on y axis) to each monkeypox antigen over serial dilution points of plasma samples (\log_{10} transformed dilution factor on x axis) collected from mice with and without vaccination of two or three doses of MPXVac-097, Mix-5 or single antigen LNP-mRNAs on day 0, 14 and 28. The single antigen LNP mRNA is matched with antigen used in the ELISA (e.g. plasma from mice vaccinated with A35R LNP mRNA will be used in A35R ELISA).

b, PRNT titration curves showing percent of plaque reduction (y axis) over serial dilution of plasma samples (\log_{10} transformed dilution factor on x axis) collected from mice on day 28 and day 0.

The sample number in each group is indicated as n in the bracket. The vaccination schedule is shown in supplementary figure 16.



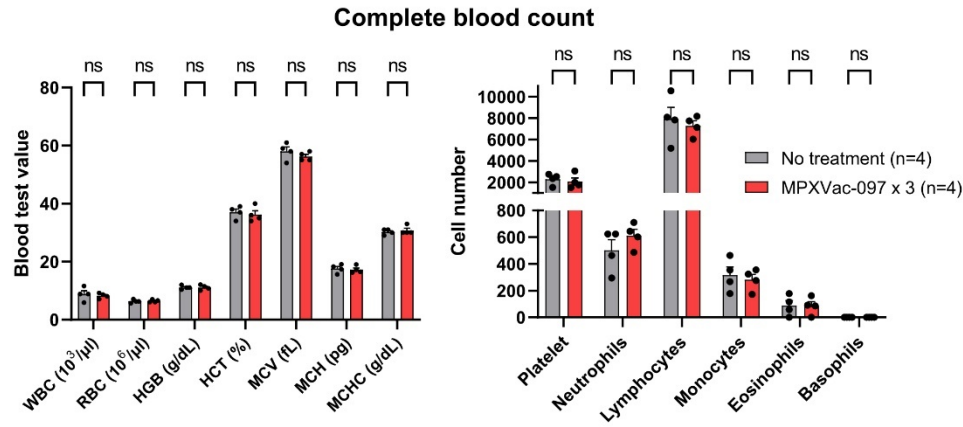
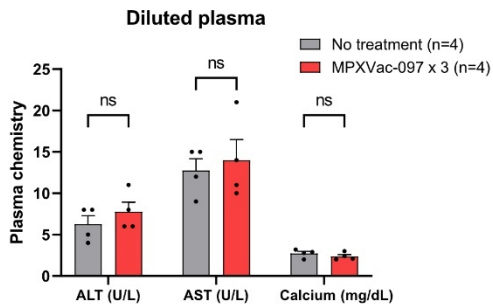
Supplementary information, Fig. S17. MPXVac-097 and Mix-5 elicit potent antibody response and protection against vaccinia virus challenge in mice.

a, ELISA quantifying binding antibody response to five monkeypox antigens in mice vaccinated with 5 μ g MPXVac-097, 5 μ g Mix-5 (equal-mass mixture of five 1 μ g single antigen LNP mRNAs) or 1 μ g single antigen LNP mRNA. Titers were measured as dilution-dependent area under curve (AUC) of dilution-response curves in Fig. S16. The single antigen vaccination group is matched with ELISA antigen tested.

b, Both MPXVac-097 and Mix-5 LNP-mRNA elicited poxvirus neutralizing antibody response (n = 5).

c, MPXVac-097 and Mix-5 vaccination offered protection against vaccinia virus challenge. Percent of clinical score of mice in each group were plotted over time (days).

Statistics: **a**, two-way ANOVA with Turkey's multiple comparison test. **b**, one-way ANOVA. **c**, one-way ANOVA with Dunnett's multiple comparison test.

a**b**

Supplementary information, Fig. S18. In vivo safety profiling of mice vaccinated with MPXVac-097.

a, Complete blood count data from mice without treatment or with three doses of 5 μg MPXVac-097.

b, Liver enzymes and calcium concentration in diluted plasma of mice with or without MPXVac-097 vaccination.

Statistics: **a-b**, two-way ANOVA with Sidak's multiple comparison test. Level of significance: * $p < 0.05$, ** $p < 0.01$, *** $p < 0.001$, **** $p < 0.0001$, and n.s., not significant. Data in plots are shown as mean \pm s.e.m. with individual data points in plots.